The Unique Developmental Differentiation in Ultra-Low Frequency Nucleus Magnocellularis

Kristine McLellan[1,2], George Ordiway[3] & Jason Tait Sanchez[1,2,3,4]

[1]Northwestern University Interdepartmental Neuroscience, [2]Department of Neurobiology, Northwestern University, Evanston, IL. USA, [3]Roxelyn and Richard Department of Communication Sciences and Disorders, [4]Knowles Hearing Research Center

Abstract

The distinct tonotopic organization of auditory brainstem neurons in the chicken nucleus magnocellularis (NM) permits the precise temporal and spatial encoding of different sound frequencies. Recent work on the most caudal-lateral, ultra-low frequency region of NM (denoted NMc) describes neurons that demonstrate structural and functional differences from their higher-frequency NM counterparts. While we have characterized the functional phenotype of NMc neurons in late-developing chicken embryos (E20-21), little is known about the properties of NMc neurons at earlier developmental stages. Using whole-cell patch clamp electrophysiology, we recorded from the most caudal-lateral region of NM in E13-14 chicken embryos, a developmental period just prior to the onset of hearing. We report here a distinct phenotype of NMc neurons that differ from both higher-frequency NM at a similar developmental period as well as more mature NMc. Early developing NMc neurons demonstrate significant differences in passive properties, such as input resistance and time constant, compared to NM neurons at the same age. NM and NMc at this developmental stage also exhibit differences in active properties, such as action potential (AP) current threshold, sodium current magnitude, and AP firing properties to square-pulse and sinusoidal somatic current injections. In addition to active and passive differences, a subset of NMc neurons demonstrate intrinsic spontaneous activity in the absence of synaptic contribution. While this is similar to mature NMc neurons, the spontaneity in younger neurons is broader in frequency distribution. Additionally, the total proportion of spontaneously active neurons in early-developing NMc is lower than in mature NMc, suggesting intrinsic developmental changes that work to increase spontaneity in maturation. Taken together, our results identify the NMc phenotype in embryonic stages before the onset of hearing; in doing so, we demonstrate distinctions between early- and late-developing NMc and raise questions about how and why such differences arise.

Background

TABLE 1 | Maturation of membrane, action potential, potassium current and sodium current properties.

	E10–E12	E14–E16	E19–E21
Membrane properties			
RMP (mV)	−62.21 ± 10.31 (22)	−66.33 ± 6.87 (21)	−66.52 ± 8.49 (28)
Time constant tau (ms)	15.57 ± 6.23 (10)	5.90 ± 3.26 (13)	3.18 ± 1.33 (20)
Input resistance (MΩ)	324.60 ± 120.30 (10)	211.40 ± 49.87 (13)	123.90 ± 49.90 (20)
Cell capacitance (pF)	47.91 ± 4.61 (10)	26.78 ± 9.97 (13)	26.15 ± 4.60 (20)
Action potential (AP) properties			
Threshold current (pA)	121.30 ± 80.30 (22)	242.70 ± 68.58 (21)	321.70 ± 121.00 (28)
Latency (ms)	19.49 ± 10.86 (22)	4.17 ± 1.15 (21)	3.00 ± 0.57 (28)
Max rise rate (mV/ms)	38.59 ± 12.13 (22)	98.76 ± 40.98 (21)	155.60 ± 42.19 (28)
Max fall rate (mV/ms)	−19.26 ± 5.78 (22)	−56.30 ± 25.85 (21)	−104.40 ± 29.79 (28)
AP half width (ms)	4.57 ± 1.07 (21)	1.91 ± 0.93 (21)	0.97 ± 0.17 (28)
AP reliability range (ms)	8.89 ± 8.98 (22)	0.44 ± 0.24 (21)	0.21 ± 0.14 (28)
AP height (mV)§	69.09 ± 11.64 (22)	80.27 ± 8.83 (21)	82.94 ± 9.97 (28)
K_V current (I_k)			
Total I_k at +20 mV (pA)	3076 ± 1272 (35)	4386 ± 1105 (42)	6240 ± 1327 (39)
Total I_k conductance (nS)	26.99 ± 11.16 (35)	38.47 ± 9.70 (42)	54.74 ± 11.64 (39)
Total I_k density (pA/pF)	71.71 ± 26.75 (10)	172.00 ± 65.47 (13)	258.60 ± 65.62 (15)
Na_V current (I_{Na})			
$V_{25\%}$ (mV)^	−33.64 ± 4.99 (14)	−40.50 ± 5.57 (24)	−50.36 ± 6.02 (11)
I_{Na} (pA)*	−1728.00 ± 759.10 (14)	−2453.00 ± 654.00 (24)	−3386.00 ± 1089.00 (11)
I_{Na} conductance (nS)*	24.15 ± 8.90 (14)	32.43 ± 7.51 (24)	44.97 ± 12.07 (11)
I_{Na} density (pA/pF)*	−36.17 ± 13.99 (12)	−84.16 ± 48.52 (20)	−98.59 ± 53.48 (10)
Max rise rate (pA/ms)*	−4223.00 ± 2906.00 (14)	−7836.00 ± 3837.00 (24)	−10546.00 ± 5736.00 (11)
Max fall rate (pA/ms)*	1008.00 ± 735.00 (14)	1842.00 ± 776.80 (24)	2782.00 ± 1117.00 (11)
Half width (ms)*	1.99 ± 1.03 (14)	1.29 ± 0.37 (24)	1.13 ± 0.14 (11)
Reliability range (ms)*	0.46 ± 0.42 (22)	0.39 ± 0.39 (23)	0.50 ± 0.42 (18)
$V_{1/2}$ (mV)	−49.87 ± 3.20 (7)	−47.13 ± 5.27 (8)	−54.67 ± 3.77 (7)

Table 1. Passive and active properties across developmental periods of chicken NM neurons. Table adopted from Hong et al. (2016), Frontiers in Cellular Neuroscience. 10:80, 1-22.

Methods

Acute brainstem slices were prepared from White Leghorn chicken (Gallus gallus domesticus) at embryonic (E) days E13-E14. Whole-cell current and voltage clamp recordings were obtained from NMc neurons in the most caudal slices containing NM. Current steps and voltage commands of varying durations, strengths, and frequencies were injected into the soma of NMc neurons using an Axon Multiclamp 700B amplifier. Results were acquired and analyzed using Clampfit 11.0 analysis software.

Funding: NIH, NIDCD R01 DC017167 (JTS)
The School of Communication and The Knowles Hearing Research Center, Northwestern University

Early vs. Late-Developing NMc

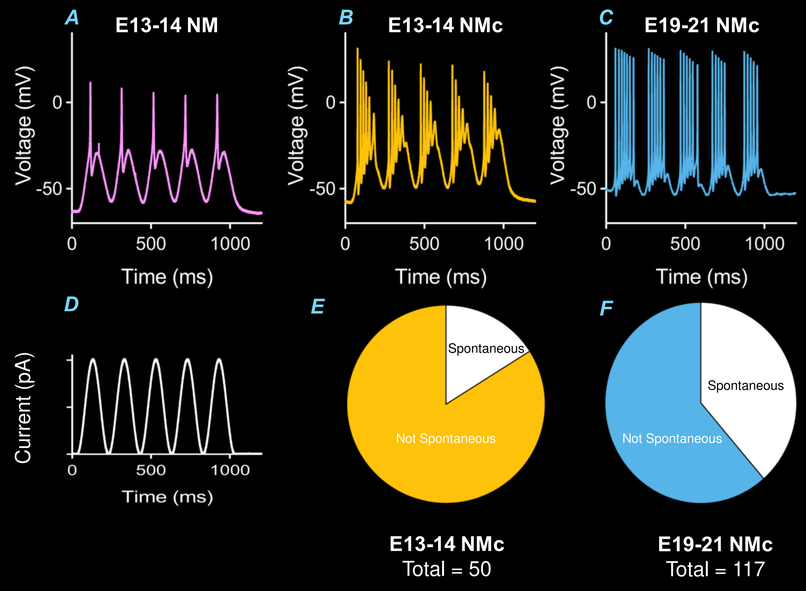

Figure 1: Responses to sinusoidal current injections. Voltage responses of representative early-developing NM (A), early-developing NMc (B), and late developing NMc (C) neurons from a 5Hz sinusoidal current injection (200 pA) (D). Some NMc neurons exhibit intrinsic spontaneous activity, though the E13-14 (E) NMc neurons show a lower proportion of these compared to E19-21 NMc (F).

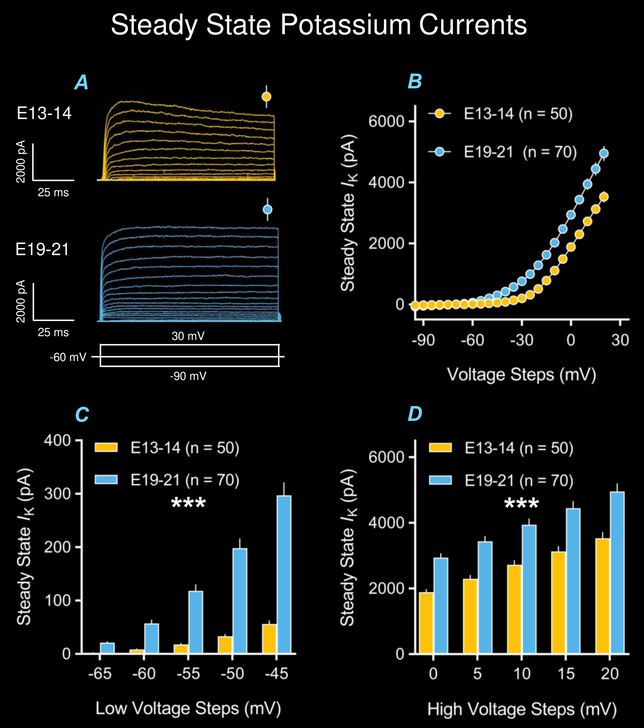

Figure 2: Outward steady state (SS) potassium currents (I_k) are significantly different at each voltage above RMP. (A) Representative I_K current traces from early- (top) and late- (bottom) developing NMc neurons. Circles denote the steady-state I_k value. (B) Steady state I_k from early- and late-developing neurons across voltage steps. Significant differences in low-voltage activated (C) and high-voltage activated (D) I_k currents are enlarged. ***p<0.05 for all comparisons in the graphs.

Passive Membrane Properties

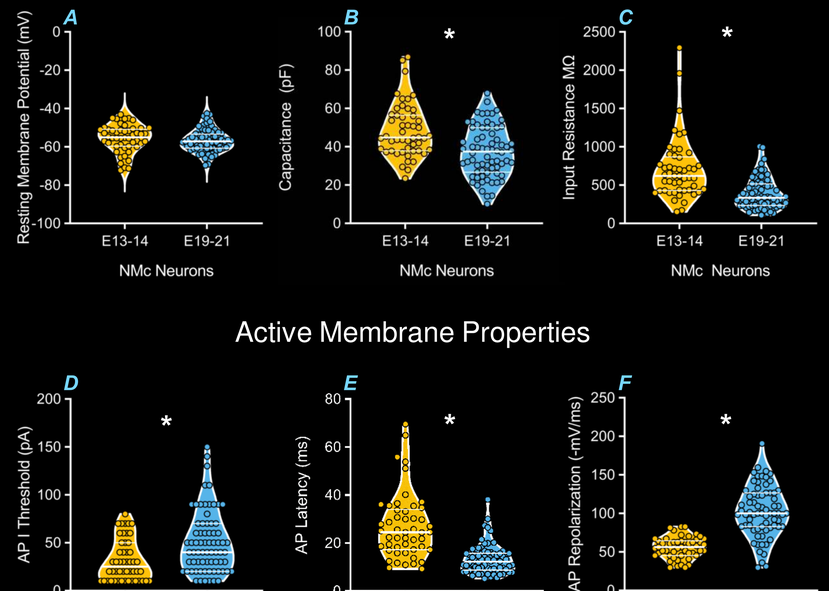

Active Membrane Properties

Figure 3: NMc neuronal membrane properties. Passive membrane properties: resting membrane potential *(A)*, capacitance *(B)*, and input resistance *(C)* early- and late-developing NMc neurons. Active membrane properties: action potential (AP) current threshold *(D)*, AP latency *(E)*, and AP repolarization rate *(F)* for the same neurons. In this figure, *$p < 0.05$.

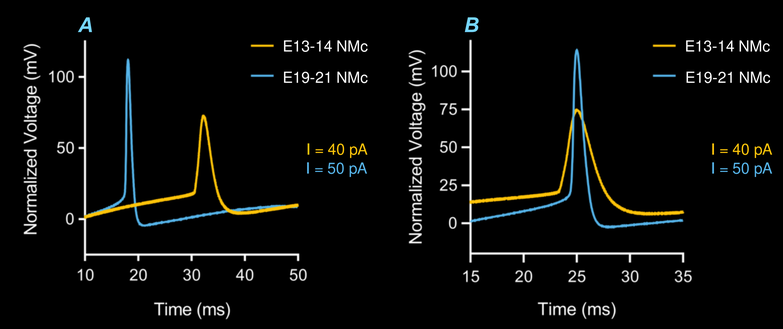

Figure 4: Differences between early- and late- developing NMc action potentials. (A) Representative traces from a suprathreshold current injection (125% above current threshold) for ages E13-14 and E19-21 NMc highlight their differences in threshold, latency, and peak. (B) The same action potentials with peaks overlaid demonstrate the lengthened repolarization rate of early-developing NMc neurons compared to their late-developing counterparts.

Conclusions

1. A distinct NMc phenotype exists at the early-developing ages of E13-14 and differs from NM and more mature NMc neurons. Spontaneously-active neurons are also present at a lower prevalence in E13-14 versus E19-21 NMc neurons.
2. Early-developing NMc neurons had significantly smaller low-voltage activated and high-voltage activated potassium currents compared to late-developing NMc.
3. Lower levels of total steady state I_k likely caused early-developing NMc neurons to have a higher input resistance, lower AP current threshold, longer AP latency, and slower repolarization rate compared to their late-developing counterparts. E13-14 NMc neurons also exhibited a larger capacitance on average compared to ages E19-21, likely due to a larger soma and broader dendritic architecture.